Inorg. Chem. **1993,** *32,* 2183-2189

Mixed Platinum(II)-Mercury(II) Cytosine Nucleobase Complexes with Metal-Metal Bonds[†]

Michael Krumm,[1a] Ennio Zangrando,[1b] Lucio Randaccio,[*,1b] Stephan Menzer,[1a] Annette Danzmann,[1a] Dagmar Holthenrich,[1a] and Bernhard Lippert[*,1a]

Fachbereich Chemie, Universität Dortmund, D-4600 Dortmund, Germany, and Dipartimento di Scienze Chimiche, Università di Trieste, 34127 Trieste, Italy

Received September 15, 1992

Reaction of *trans*-$[a_2PtL_2]^{2+}$ (a = NH_3 or CH_3NH_2; L = 1-methylcytosine, $C_5H_7N_3O$, or 1,5-dimethylcytosine, $C_6H_9N_3O$) with HgO in water yields novel heteronuclear Pt–Hg compounds containing two bridging cytosyl ligands L^-, binding to Pt via N3 and to Hg via the deprotonated exocyclic amino group N4. Three representative examples have been characterized by X-ray crystallography: *trans*-$[(CH_3NH_2)_2Pt(1\text{-}MeC^-)_2Hg](NO_3)_2$ (**1d**), *trans*-$[(CH_3NH_2)_2Pt(1,5\text{-}DimeC^-)_2Hg](NO_3)_2 \cdot 0.5H_2O$ (**2d**), and *trans*-$[(CH_3NH_2)_2Pt(1\text{-}MeC^-)_2Hg]Cl(NO_3)$ (**1e**). Crystal data are as follows: **1d**, triclinic system, space group $P\bar{1}$, a = 10.157(4) Å, b = 10.494(4) Å, c = 11.452(4) Å, α = 101.33(2)°, β = 102.44(2)°, γ = 104.65(2)°, V = 1111.8(7) Å^3, Z = 2; **1e**, monoclinic system, space group $C2/m$, a = 13.876(4) Å, b = 16.254(3) Å, c = 10.358(3) Å, β = 112.02(1)°, V = 2166(1) Å^3, Z = 4; **2d**, monoclinic system, space group $P2_1/n$, a = 8.614(3) Å, b = 20.610(6) Å, c = 13.984(5) Å, β = 97.67(2)°, V = 2461(2) Å^3, Z = 4. In all three compounds, Pt displays a square-pyramidal coordination sphere, with Hg in the apical position. Hg has severely distorted coordinations with two short Hg–N(4) distances, a Hg–Pt contact, and longer $Hg\text{–}O_3N^-$ distances in **1d** (distorted octadedron) and **2d** (distorted bipyramid), whereas in **1e** the coordination around Hg is completed by Cl^- (distorted bipyramid). Pt–Hg separations are 2.785(1) Å (**1d**), 2.765(1) Å (**2d**), and 2.835(1) Å (**1e**), and interactions are interpreted in terms of weak Pt–Hg bonds. The ^{195}Pt NMR spectra of the Pt–Hg compounds display ^{199}Hg satellites due to ^1J coupling, consistent with Pt–Hg bonding. ^1H NMR spectra of the various Pt–Hg compounds show ^{195}Pt and ^{199}Hg coupling, as determined by decoupling and spectral editing techniques. Unlike related Pt–Pt compounds, the mixed-metal Pt–Hg species, when reacted with a large variety of N and S donor ligands X, tend to decompose with formation of *trans*-$[a_2PtL_2]^{2+}$ and HgX_2.

Introduction

Metal–metal bonding in heteronuclear complexes containing both d^8 and d^{10} metal ions has been known for some 25 years.[2,3] A rich chemistry has been established for such species, in particular for the following combinations: Ir^I and Au^I,[4] Ir^I and Ag^I,[5,6] Pt^{II} and Hg^{II},[7-9] Pt^{II} and Ag^I,[10-13] and Pt^{II} and Au^I,[14,15] as well as Rh^I and Ag^I.[16] Our interest in metal and mixed-metal nucleobase complexes[17] has led us, among others, also to heteronuclear complexes[18] containing the *cis*-$(NH_3)_2Pt^{II}$ entity, the d^{10} metal ions Ag^I [19-21] and Zn^{II},[22] and bridging 1-methyluracil, 1-methylthymine, and 1-methylcytosine nucleobases. Despite reasonably

---

[†] Dedicated to Prof. Heinrich Nöth.

(1) (a) Universität Dortmund. (b) Università di Trieste.

(2) Coffey, E.; Lewis, J.; Nyholm, R. S. *J. Chem. Soc.* **1964**, 1741.

(3) Kuyper, J.; Vrieze, K. *J. Organomet. Chem.* **1976**, *107*, 129.

(4) (a) Balch, A. L.; Catalano, V. J. *Inorg. Chem.* **1991**, *30*, 1302. (b) Balch, A. L.; Catalano, V. J.; Olmstead, M. M. *J. Am. Chem. Soc.* **1990**, *112*, 2010. (c) Balch, A. L.; Oram, D. E.; Reedy, P. E., Jr. *Inorg. Chem.* **1987**, *26*, 1837. (d) Balch, A. L.; Nagle, J. K.; Oram, D. E.; Reedy, P. E., Jr. *J. Am. Chem. Soc.* **1988**, *110*, 454.

(5) (a) Liston, D. J.; Reed, C. A.; Eigenbrot, C. W.; Scheidt, W. R. *Inorg. Chem.* **1987**, *26*, 2739. (b) Liston, D. J.; Lee, Y. J.; Scheidt, W. R.; Reed, C. A. *J. Am. Chem. Soc.* **1989**, *111*, 6643.

(6) (a) Sykes, A. G.; Mann, K. R. *J. Am. Chem. Soc.* **1990**, *112*, 7247. (b) Sykes, A. G.; Mann, K. R. *Inorg. Chem.* **1990**, *29*, 4449. (c) Sykes, A. G.; Mann, K. R. *J. Am. Chem. Soc.* **1988**, *110*, 8252; **1990**, *112*, 1297.

(7) Kuyper, J. *Inorg. Chem.* **1978**, *17*, 1458.

(8) (a) van der Ploeg, A. F. M. J.; van Koten, G.; Vrieze, K.; Speck, A. L. *Inorg. Chem.* **1982**, *21*, 2014 and references therein. (b) van der Ploeg, A. F. M. J.; van Koten, G.; Vrieze, K.; Spek, A. L.; Duisenberg. A. J. M. *Organometallics* **1982**, *1*, 1066.

(9) There are many more examples of mixed Hg–Pt complexes in other oxidation states. See, e.g.: (a) Albinati, A.; Moor, A.; Pregosin, P. S.; Venenzi, L. M. *J. Am. Chem. Soc.* **1982**, *104*, 7672. (b) Rossell, O.; Seco, M.; Torra, I.; Solans, X.; Font-Altaba, M. *J. Organomet. Chem.* **1984**, *270*, C63. (c) Ghilardi, C. A.; Midollini, S.; Moneti, S.; Orlandini, A.; Scapacci, G.; Dakternieks, D. *J. Chem. Soc., Chem. Commun.* **1989**, 1696. (d) Schoettel, G.; Vittal, J. J.; Puddephatt, R. J. *J. Am. Chem. Soc.* **1990**, *112*, 6400.

(10) (a) van der Ploeg, A. F. M. J.; van Koten, G.; Vrieze, K. *Inorg. Chem.* **1982**, *21*, 2026. (b) van der Ploeg, A. F. M. J.; van Koten, G.; Brevard, C. *Inorg. Chem.* **1982**, *21*, 2878.

(11) Connelly, N. G.; Lucy, A. R.; Payne, J. D.; Galas, A. M. R.; Geiger, W. E. *J. Chem. Soc., Chem. Commun.* **1983**, 1879.

(12) (a) Arsenault, G. J.; Anderson, C. M.; Puddephatt, R. J. *Organometallics* **1988**, *7*, 2094. (b) Rochon, F. D.; Melanson, R. *Acta Crystallogr.* **1988**, *C44*, 474.

(13) (a) Usón, R.; Forniés, J.; Tomás, M.; Ara, I.; Casas, J. M.; Martin, A. *J. Chem. Soc., Dalton Trans.* **1991**, 2253. (b) Usón, R.; Forniés, J.; Tomás, M.; Casas, J. M. *Angew. Chem., Int. Ed. Engl.* **1989**, *28*, 748. (c) Usón, R.; Forniés, J.; Tomás, M.; Ara, I.; Casas, J. M. *Inorg. Chem.* **1989**, *28*, 2388. (d) Cotton, F. A.; Falvello, L. R.; Usón, R.; Forniés, J.; Tomás, M.; Casas, J. M.; Ara, I. *Inorg. Chem.* **1987**, *26*, 1366. (e) Usón, R.; Forniés, J.; Tomás, M.; Casas, J. M.; Cotton, F. A.; Falvello, L. R. *Inorg. Chem.* **1987**, *26*, 3482. (f) Usón, R.; Forniés, J.; Tomás, M.; Casas, J. M.; Cotton, F. A.; Falvello, L. R. *Inorg. Chem.* **1986**, *25*, 4519. (g) Usón, R.; Forniés J.; Tomás, M.; Casas, J. M.; Cotton, F. A.; Falvello, L. R. *Polyhedron* **1986**, *5*, 901. (h) Usón, R.; Forniés, J.; Menjón, B.; Cotton, F. A.; Falvello, L. R.; Tomás, M. *Inorg. Chem.* **1985**, *24*, 4651.

(14) Yip, H.-K.; Che, C.-M.; Peng, S.-M. *J. Chem. Soc., Chem. Commun.* **1991**, 1626.

(15) (a) Murray, H. H.; Briggs, D. A.; Garzon, G.; Raptis, R. G.; Porter, L. C.; Fackler, J. P., Jr. *Organometallics* **1987**, *6*, 1992. (b) King, C.; Heinrich, D. D.; Garzon, G.; Wang, J.-C.; Fackler, J. P., Jr. *J. Am. Chem. Soc.* **1989**, *111*, 2300.

(16) Nyholm, R. S.; Vrieze, K. *J. Chem. Soc.* **1965**, 5357.

(17) Lippert, B. *Prog. Inorg. Chem.* **1989**, *37*, 1.

(18) (a) Lippert, B. In *Metal-Based Anti-Tumour Drugs*; Gielen, M. F., Ed.; Freund: London, 1988; p 201. (b) Lippert, B. In *Handbook of Nucleobase Complexes*; Lusty, J. R., Ed.; CRC Press: Boca Raton, FL, 1990; Vol. 1, p 9. (c) Goodgame, M.; Jakubovic, D. A. *Coord. Chem. Rev.* **1987**, *79*, 97.

(19) (a) Lippert, B.; Neugebauer, D. *Inorg. Chim. Acta* **1980**, *46*, 171. (b) Lippert, B.; Neugebauer, D. *Inorg. Chem.* **1982**, *21*, 451. (c) Thealt, U.; Neugebauer, D.; Lippert, B. *Inorg. Chem.* **1984**, *23*, 1713. (d) Lippert, B.; Schöllhorn, H.; Thewalt, U. *Inorg. Chem.* **1987**, *26*, 1736. (e) Goodgame, D. M. L.; Rollins, R. W.; Lippert, B. *Polyhedron* **1985**, *4*, 829.

(20) (a) Schöllhorn, H.; Thewalt, U.; Lippert, B. *J. Chem. Soc., Chem. Commun.* **1984**, 769. (b) Dieter, I.; Lippert, B.; Schöllhorn, H.; Thewalt, U. *Z. Naturforsch.* **1990**, *45B*, 731.

(21) Schöllhorn, H.; Thewalt, U.; Lippert, B. *Inorg. Chim. Acta* **1987**, *135*, 155.

(22) Schöllhorn, H.; Thewalt, U.; Lippert, B. *Inorg. Chim. Acta* **1985**, *108*, 77.

0020-1669/93/1332-2183$04.00/0

short metal–metal distances (2.760(1) Å in the Pt–Zn complex,[22] 2.787(1)–2.906(1) Å in the various Pt–Ag compounds[19–21]), we have been reluctant to use the term metal–metal bond in these compounds, primarily because of the inherent donor properties of the bridging nucleobase(s), which we considered more significant than the donor properties of the d^8 metal Pt^{II}.[23] Only in one case,[19d] with a [Pt^{II}]$_2$ dinuclear complex being oxidized by Ag^I, was there some indirect evidence to postulate an intermediate with a Pt–Ag bond.

Very recently,[24] we discovered strong metal–metal bonding between the two d^8 metal ions Pt^{II} and Pd^{II} in dinuclear nucleobase complexes of composition *trans*-$[a_2Pt(L^-)_2PdY]^{n+}$ (a = NH$_3$, CH$_2$NH$_3$; L$^-$ = 1-methylcytosyl; Y = variable ligand). In these compounds, the two metal coordination planes are perpendicular to each other, with Pt acting as a ligand of Pd. Using the same ligand system *trans*-$[a_2PtL_2]^{2+}$ and extending it to L = 1,5-dimethylcytosine, we decided to also study reactions with the d^{10} metal ion Hg^{II}. Herein, we report on preparative, structural, and NMR spectroscopic studies of such heteronuclear complexes.

Experimental Section

The starting materials *trans*-$[a_2PtL_2]X_2$ (a = NH$_3$, L = 1-MeC, X = NO$_3$ (**1a**); a = CH$_3$NH$_2$, L = 1-MeC, X = NO$_3$ (**1b**)) were prepared as described previously.[24b,25] *trans*-$[a_2PtL_2]X_2$ (a = NH$_3$, L = 1,5-DimeC, X = NO$_3$ (**2a**); a = CH$_3$NH$_2$, L = 1,5-DimeC, X = NO$_3$ (**2b**)) were prepared in analogy to **1a** and **1b** with 1,5-DimeC obtained from Chemogen, Konstanz, Germany. Yields were 77% (**2a**) and 67% (**2b**). Expectedly, all compounds were colorless. Anal. Calcd (found) for $C_{12}H_{24}N_{10}O_8Pt$ (**2a**): C, 22.8 (22.7); H, 3.8 (3.8); N, 22.2 (22.0). Calcd (found) for $C_{14}H_{28}N_{10}O_8Pt$ (**2b**): C, 25.5 (25.4); H, 4.3 (4.3); N, 21.2 (21.2). IR (cm^{-1}) for **2a**: 1655 vs, 1617 vs, 1530 vs, 1490 s, 1380 vs, 1330 s, 825 m, 775 m. IR (cm^{-1}) for **2b**: 1656 vs, 1615 vs, 1535 vs, 1500 s, 1375 vs, 1310 m, 830 m, 780 m.

Preparation of the Mixed-Metal Compounds. The heteronuclear complexes (Pt–Hg) were prepared as follows: *trans*-$[a_2PtL_2](NO_3)_2$ (0.17 mmol) was dissolved in water (25 mL), HgO (0.17 mmol) was added, and the initially orange suspension (pH 5.8) was stirred at 65 °C for 18 h. The then colorless solution was concentrated to a small volume (5 mL) by rotary evaporation and allowed to slowly evaporate at 22 °C in an open beaker. Colorless cubes were harvested in all cases, washed with 1 mL of cold water, and dried in air. **1e** was obtained upon recrystallization (H$_2$O) of **1d** in the presence of a 6-fold excess of NaCl.

***trans*-$[(NH_3)_2Pt(1\text{-}MeC^-)_2Hg](NO_3)_2\cdot 2H_2O$ (1c).** Anal. Calcd (found) for $C_{10}H_{22}N_{10}O_{10}PtHg$: C, 14.3 (14.2); H, 2.6 (2.7); N, 16.8 (17.2). Yield: 80%. IR (cm^{-1}): 1650 vs, 1540 vs, 1495 s, 1390 s, 1310 w.

***trans*-$[(CH_3NH_2)_2Pt(1\text{-}MeC^-)_2Hg](NO_3)_2$ (1d).** Anal. Calcd (found) for $C_{12}H_{22}N_{10}O_8PtHg$: C, 17.4 (17.5); H, 2.7 (2.7); N, 16.9 (17.0). Yield: 70%. IR (cm^{-1}): 1643 vs, 1527 vs, 1493 s, 1435 m, 1385 vs, 1310 s, 770 m.

***trans*-$(CH_3NH_2)_2Pt(1\text{-}MeC^-)_2HgCl(NO_3)$ (1e).** Anal. Calcd (found) for $C_{12}H_{22}N_9O_5ClPtHg$: C, 17.9 (17.7); H, 2.8 (3.0); N 15.7 (15.5). Yield: 95%. IR (cm^{-1}): 1645 vs, 1519 vs, 1486 s, 1451 s, 1430 vs, 1384 vs, 1355 s, 1336 s, 808 m, 765 m, 486 m.

***trans*-$[(NH_3)_2Pt(1,5\text{-}DimeC^-)_2Hg](NO_3)_2\cdot 5H_2O$ (2c).** Anal. Calcd (found) for $C_{12}H_{32}N_{10}O_{13}PtHg$: C, 15.7 (15.9); H, 3.4 (3.0); N, 15.2 (15.0). Yield: 59%. IR (cm^{-1}): 1660 s, 1620 s, 1580 m, 1430 vs, 810 m.

***trans*-$[(CH_3NH_2)_2Pt(1,5\text{-}DimeC^-)_2Hg](NO_3)_2\cdot 0.5H_2O$ (2d).** Anal. Calcd (found) for $C_{14}H_{27}N_{10}O_{8.5}PtHg$: C, 19.4 (19.3); H, 3.1 (3.2); N, 16.2 (15.9). Yield: 64%. IR (cm^{-1}): 1670 vs, 1645 vs, 1520 vs, 1390 s, 1370 s, 770 m.

***trans*-$[(CH_3NH_2)_2Pt(1\text{-}MeC^-)_2Hg(SCN)]NO_3$ (1f)** was obtained as a colorless precipitate upon addition of 1 equiv of NaSCN to an aqueous solution of **1d** (0.078 mmol each in 10 mL) in 70% yield. Anal. Calcd (found) for $C_{13}H_{22}N_{10}O_5SPtHg$: C, 18.9 (18.4); H, 2.7 (2.7); N, 17.0 (17.0). IR (cm^{-1}): 2089 vs, 1647 vs, 1526 vs, 1485 s, 1434 s, 1395 s, 1331 s, 1279 s. Raman (cm^{-1}): 1033 s.

Table I. List of Compounds and Numbering Scheme

trans-$[(NH_3)_2Pt(1\text{-}MeC_2)](NO_3)_2$	**1a**
trans-$[(CH_3NH_2)_2Pt(1\text{-}MeC)_2](NO_3)_2$	**1b**
trans-$[(NH_3)_2Pt(1\text{-}MeC^-)_2Hg](NO_3)_2\cdot 2H_2O$	**1c**
trans-$[(CH_3NH_2)_2Pt(1\text{-}MeC^-)_2Hg](NO_3)_2$	**1d**
trans-$(CH_3NH_2)_2Pt(1\text{-}MeC^-)_2HgCl(NO_3)$	**1e**
trans-$[(CH_3NH_2)_2Pt(1\text{-}MeC^-)_2Hg(SCN)]NO_3$	**1f**
trans-$[(NH_3)_2Pt(1,5\text{-}DimeC)_2](NO_3)_2$	**2a**
trans-$[(CH_3NH_2)_2Pt(1,5\text{-}DimeC)_2](NO_3)_2$	**2b**
trans-$[(NH_3)_2Pt(1,5\text{-}DimeC^-)_2Hg](NO_3)_2\cdot 5H_2O$	**2c**
trans-$[(CH_3NH_2)_2Pt(1,5\text{-}DimeC^-)_2Hg](NO_3)_2\cdot 0.5H_2O$	**2d**

Table I provides a list of compounds prepared.

Instrumentation. IR spectra (KBr pellets) were recorded on Perkin-Elmer 580B and Bruker IFs 113v FT spectrometers; Raman spectra, on a Coderg T800 with argon (514.5 nm) or krypton laser (647.1 nm) excitation. ^{1}H, ^{195}Pt, and ^{199}Hg NMR spectra (200.13, 42.95, 35.79 MHz; 5-mm tubes; $c \approx 0.1$ M; ambient temperature) were recorded with a Bruker AC 200 instrument. Chemical shifts are given in ppm and are referenced to internal TSP (^{1}H), external Na$_2$PtCl$_6$ (^{195}Pt), and external Me$_2$Hg (^{199}Hg), respectively. Assignment of the x-nuclei satellites in proton NMR spectra, as well as the determination of the ^{199}Hg chemical shifts, was made by 1D and 2D ^{1}H–^{199}Hg HMQC[26] and ^{1}H–^{195}Pt HMQC experiments, without decoupling during acquisition. The sequence was optimized to $^5J(^{199}Hg\text{–}^1H) \approx 23$ Hz, $^2J(^{199}Hg\text{–}^1H) \approx 26$ Hz, $^4J(^{195}Pt\text{–}^1H) \approx 20$ Hz, and $^3J(^{195}Pt\text{–}^1H) \approx 38$ Hz. $^1H\{^{195}Pt\}$ spectra were recorded using GARP1[27] (4-kHz field strength) and the inverse mode of the instrument.

X-ray Crystallography. The following compounds were studied by X-ray crystallography: *trans*-$[(CH_3NH_2)_2Pt(1\text{-}MeC^-)_2Hg](NO_3)_2$ (**1d**), *trans*-$[(CH_3NH_2)_2$ $Pt(1,5\text{-}DimeC^-)_2Hg](NO_3)_2\cdot 0.5H_2O$ (**2d**) and *trans*-$(CH_3NH_2)_2Pt(1\text{-}MeC^-)_2$ $HgCl(NO_3)$ (**1e**).

Unit cell dimensions were determined from Weissenberg and precession photographs and refined from 25 reflections in the θ range 13–19° on a CAD4 Enraf-Nonius single crystal diffractometer using graphite-monochromated Mo Kα (λ = 0.7107 Å) radiation. In all the structures, reflections with $I > 3(I)$ were corrected for Lorentz–polarization effects and for secondary extinction. Absorption correction was applied via an empirical ψ scan of all the structures. The structures were solved by conventional Patterson and Fourier methods and refined by full-matrix anisotropic least-squares methods to the final R and R_w values given in Table II. In **2d**, a water molecule of crystallization was found. In **1e**, the NO$_3^-$ anion was disordered in two orientations differing by 61(1)° around the N7–O7 bond. An occupancy factor of 0.5 was assigned to the water molecule (**2d**) and to O71 and O72 atoms (**1e**), on the basis of electron peak densities on the Fourier maps. The contribution of hydrogen atoms, kept in calculated positions ($B = 1.3B_{eq}$ of the corresponding bonded atoms), were included in the final refinement, except for hydrogen atoms of water molecule Ow in **2d**. Crystallographic data and details of refinements are reported in Table II. All calculations were carried out on a MicroVAX 2000 computer with the Enraf-Nonius package.[28] Fractional atomic coordinates and equivalent isotropic thermal parameters are reported in Tables III–V.

Results

Ligands and Starting Compounds. 1-MeC and 1,5-DimeC are models of the naturally occurring cytosine and 5-methylcytosine nucleobases. 5-Methylcytosine occurs not only in tRNAs but also in DNA. The amount of 5-methylated cytosine in DNA appears to be inversely correlated with transcriptional activity. Our choice for 1,5-DimeC as a ligand resulted from observations of a hydrolytic deamination of 1-MeC ligands in *trans*-$[a_2Pt(1\text{-}MeC)_2]^{2+}$ under basic pH conditions to give the corresponding 1-methyluracil (1-MeU) complex.[29] The use of 1,5-DimeC instead of 1-MeC yielded the bis(1-methylthyminate) complex, as expected.

Like *trans*-$[a_2Pt(1\text{-}MeC)_2]^{2+}$,[24b,30] *trans*-$[a_2Pt(1,5\text{-}DimeC)_2]^{2+}$ (a = NH$_3$ (**2a**), CH$_3$NH$_2$ (**2b**)) exists in solution as two rotamers,

---

[23] With related trinuclear complexes PtMPt (M = Cu^{II}, Ni^{II}, Fe^{II}), Pt^{II} was considered a weak σ donor via filled d$_{z^2}$ orbitals. Cf.: Goodgame, D. M. L.; Hitchman, M. A.; Lippert, B. *Inorg. Chem.* **1986**, *25*, 2191.

[24] (a) Krumm, M.; Lippert, B.; Randaccio, L.; Zangrando, E. *J. Am. Chem. Soc.* **1991**, *113*, 5129. (b) Krumm, M.; Zangrando, E.; Randaccio, L.; Menzer, S.; Lippert, B. *Inorg. Chem.* **1993**, *32*, 700.

[25] Lippert, B.; Lock, C. J. L.; Speranzini, R. A. *Inorg. Chem.* **1981**, *20*, 808.

[26] Bax, A.; Griffey, R. H.; Hawkins, B. L. *J. Magn. Reson.* **1983**, *55*, 301.

[27] Shaka, I. S.; Barker, P. B.; Freeman, R. *J. Magn. Reson.* **1985**, *64*, 547.

[28] Frenz, B. A. Enraf-Nonius Structure Determination Package. B. A. Frenz and Associates, College Station, TX 77840, and Enraf-Nonius, Delft, The Netherlands.

[29] Krumm, M.; Erxleben, A.; Lippert, B. Unpublished results.

[30] Krizanovic, O.; Pesch, F. J.; Lippert, B. *Inorg. Chim. Acta* **1989**, *165*, 145.

Table II. Crystallographic Data and Details of Refinements for Compounds **1d**, **2d**, and **1e** (298 K; Mo Kα Radiation (λ = 0.7107 Å))

	1d	**2d**	**1e**
empirical formula	$C_{12}H_{22}HgPtO_8N_{10}$	$C_{14}H_{26}HgPtO_8N_{10}\cdot 0.5H_2O$	$C_{12}H_{22}HgPtClO_5N_9$
fw	830.0	867.1	803.5
a, Å	10.157(4)	8.614(3)	13.876(4)
b, Å	10.494(4)	20.610(6)	16.254(3)
c, Å	11.452(4)	13.984(5)	10.358(3)
α, deg	101.33(2)		
β, deg	102.44(2)	97.67(2)	112.02(1)
γ, deg	104.65(2)		
V, Å^3	1111.8(7)	2461(2)	2166(1)
D_{calc}, g cm^{-3}	2.48	2.34	2.46
Z	2	4	4
crystal system	triclinic	monoclinic	monoclinic
space group	$P\bar{1}$ (No. 2)	$P2_1/n$ (No. 14, cell choice 2)	$C2/m$ (No. 12)
μ(Mo Kα), cm^{-1}	133.0	120.3	137.6
F(000)	772	1628	1488
2θ max, deg	58	56	56
no. of reflcns measd	6177	6336	2852
absorption	ψ scan	ψ scan	ψ scan
% transm: max, min	99.9, 36.5	99.8, 18.5	99.4, 33.6
no. of obs, $I \geq 3\sigma(I)$	3259	3850	2103
no. of variables	290	317	153
weighting scheme	unit	unit	unit
$R(F_o)$	0.058	0.055	0.027
$R_w(F_o)$	0.062	0.058	0.029

Table III. Atomic Positional Parameters for Compound **1d**

atom	x	y	z	B,[a] Å^2
Pt	0.40666(7)	0.39937(7)	0.28230(6)	3.63(1)
Hg	0.19039(9)	0.18244(8)	0.10939(8)	5.14(2)
O2	0.716(1)	0.440(1)	0.416(1)	5.2(3)
N1	0.751(2)	0.240(2)	0.345(2)	5.7(4)
N3	0.525(1)	0.269(1)	0.280(1)	4.0(3)
N4	0.341(2)	0.086(2)	0.136(2)	5.8(4)
C1	0.904(2)	0.299(2)	0.416(2)	7.3(7)
C2	0.664(2)	0.321(2)	0.349(2)	4.7(4)
C4	0.473(2)	0.139(2)	0.207(2)	4.8(4)
C5	0.566(2)	0.055(2)	0.207(2)	7.1(6)
C6	0.700(2)	0.110(2)	0.277(2)	6.6(6)
O2a	0.436(1)	0.696(1)	0.391(1)	5.1(3)
N1a	0.225(2)	0.722(1)	0.315(2)	5.3(4)
N3a	0.264(1)	0.505(1)	0.265(1)	3.9(3)
N4a	0.081(2)	0.319(2)	0.128(2)	5.9(5)
C1a	0.285(3)	0.870(2)	0.375(3)	7.6(7)
C2a	0.313(2)	0.642(2)	0.324(2)	4.5(4)
C4a	0.125(2)	0.446(2)	0.190(2)	4.9(4)
C5a	0.037(2)	0.534(2)	0.182(2)	6.0(6)
C6a	0.086(2)	0.665(2)	0.242(2)	5.9(5)
N11	0.478(2)	0.471(2)	0.142(1)	5.0(4)
N12	0.355(1)	0.350(1)	0.435(1)	4.1(3)
C11	0.611(2)	0.591(2)	0.199(2)	6.2(6)
C12	0.251(2)	0.217(2)	0.420(2)	7.1(6)
N7	0.312(2)	0.711(1)	0.011(2)	5.5(4)
O71	0.236(2)	0.783(2)	0.016(2)	7.8(5)
O72	0.275(2)	0.593(2)	0.011(2)	9.5(6)
O73	0.431(2)	0.751(2)	0.001(2)	10.9(6)
N8	0.074(2)	0.076(2)	–0.181(2)	5.4(4)
O81	0.031(2)	0.042(2)	–0.292(2)	9.1(5)
O82	0.173(3)	0.173(2)	–0.131(2)	13.7(8)
O83	0.023(2)	0.028(2)	–0.114(2)	13.8(7)

[a] Anisotropically refined atoms are given in the form of the isotropic equivalent displacement parameter defined as $(4/3)\sum_i\sum_j a_i a_j \beta(i,j)$.

with *head–tail* and *head–head* oriented nucleobases in 3:1 (**2a**) and 4:1 (**2b**) ratios. H6 and CH_3(5) resonances of the 1,5-DimeC ligands are split into a quartet and a doublet ($^4J \approx$ 1.1 Hz), respectively. The CH_3ND_2 resonance in **2b** displays ^{195}Pt coupling ($^3J \approx$ 40 Hz), even at 200 MHz. Chemical shifts of all compounds are given in the supplementary material.

Table IV. Atomic Positional Parameters for Compound **2d**

atom	x	y	z	B,[a] Å^2
Pt	0.55436(7)	0.50670(3)	0.17602(4)	3.27(1)
Hg	0.41134(8)	0.48181(3)	0.33779(4)	4.43(1)
O2	0.573(1)	0.6241(5)	0.0471(8)	4.7(3)
N1	0.447(2)	0.7042(6)	0.115(1)	4.2(3)
N3	0.460(1)	0.5981(6)	0.1792(9)	3.7(2)
N4	0.339(1)	0.5753(7)	0.3178(8)	3.8(3)
C1	0.482(2)	0.7504(8)	0.041(1)	4.9(4)
C2	0.497(2)	0.6412(8)	0.112(1)	4.0(3)
C4	0.379(2)	0.6171(7)	0.253(1)	3.7(3)
C5	0.328(2)	0.6851(8)	0.256(1)	4.4(4)
C6	0.368(2)	0.7248(8)	0.187(1)	4.6(4)
C7	0.244(2)	0.7084(8)	0.336(1)	5.6(4)
O2a	0.775(1)	0.4323(5)	0.0638(8)	4.8(3)
N1a	0.789(2)	0.3318(6)	0.128(1)	4.1(3)
N3a	0.632(1)	0.4142(6)	0.1871(8)	3.5(2)
N4a	0.512(2)	0.3934(7)	0.325(1)	5.2(3)
C1a	0.905(2)	0.3139(9)	0.065(1)	5.5(4)
C2a	0.733(2)	0.3948(7)	0.123(1)	4.0(3)
C4a	0.594(2)	0.3720(7)	0.256(1)	4.2(3)
C5a	0.651(2)	0.3054(8)	0.259(1)	4.3(4)
C6a	0.745(2)	0.2898(7)	0.196(1)	4.8(4)
C7a	0.607(3)	0.2585(9)	0.334(2)	6.7(5)
N11	0.755(2)	0.5329(6)	0.264(1)	4.4(3)
N12	0.369(1)	0.4808(6)	0.0770(9)	3.8(3)
C11	0.871(2)	0.5649(9)	0.213(2)	6.1(5)
C12	0.219(2)	0.460(1)	0.109(2)	7.5(6)
N7	0.053(1)	0.4160(6)	0.3266(9)	3.8(3)
O71	–0.081(2)	0.4014(8)	0.342(1)	8.5(5)
O72	0.103(2)	0.4686(8)	0.346(1)	8.7(5)
O73	0.137(2)	0.3770(8)	0.293(2)	11.6(6)
N8	0.354(2)	0.3778(7)	0.538(1)	5.2(4)
O81	0.301(2)	0.3615(6)	0.6119(9)	6.2(3)
O82	0.399(2)	0.3369(6)	0.486(1)	7.6(4)
O83	0.366(2)	0.4376(6)	0.5191(9)	6.2(3)
Ow[b]	0.359(3)	0.080(1)	0.031(1)	5.1(5)

[a] See footnote *a* of Table III. [b] Occupancy factor = 0.5.

Table V. Atomic Positional Parameters for Compound **1e**

atom	x	y	z	B,[a] Å^2
Pt	0.12707(2)	0.000	0.23973(4)	2.534(7)
Hg	0.34499(3)	0.000	0.38997(4)	3.098(8)
Cl	0.4767(2)	0.000	0.6674(3)	3.37(5)
O2	–0.0416(4)	0.1269(4)	0.1313(7)	5.8(2)
N1	0.0365(4)	0.2491(4)	0.1946(7)	3.7(1)
N3	0.1324(4)	0.1251(4)	0.2458(5)	2.5(1)
N4	0.3112(4)	0.1274(4)	0.3693(6)	3.4(1)
C1	–0.0634(6)	0.2903(5)	0.1386(9)	4.7(2)
C2	0.0383(5)	0.1649(5)	0.1858(8)	3.5(2)
C4	0.2232(5)	0.1666(4)	0.3124(7)	3.1(1)
C5	0.2185(6)	0.2544(5)	0.3174(9)	4.2(2)
C6	0.1254(6)	0.2910(5)	0.2585(8)	4.1(2)
N11	0.0925(6)	0.000	0.414(1)	3.8(2)
N12	0.1443(6)	0.000	0.0533(8)	3.0(2)
C11	0.180(1)	0.000	0.555(1)	5.6(3)
C12	0.243(1)	0.000	0.041(1)	7.4(5)
N7	0.000	0.1958(4)	0.500	2.0(1)
O7	0.000	0.2714(5)	0.500	5.4(2)
O71[b]	0.0769(9)	0.1567(9)	0.503(2)	6.8(4)
O72[b]	0.049(1)	0.157(1)	0.604(2)	7.1(4)

[a] See footnote *a* of Table III. [b] Occupancy factor = 0.5.

Structural Characterization of Mixed Pt–Hg Compounds. Dinuclear Cations. Figures 1–3 depict pairs of cations of *trans*-$[(CH_3NH_2)_2Pt(1\text{-}MeC^-)_2Hg](NO_3)_2$ (**1d**), *trans*-$[(CH_3NH_2)_2Pt(1,5\text{-}DimeC^-)_2Hg](NO_3)_2\cdot 0.5H_2O$ (**2d**), and *trans*-$(CH_3NH_2)_2Pt(1\text{-}MeC^-)_2HgCl(NO_3)$ (**1e**). Selected coordination bond lengths and angles of the compounds are listed in Table VI. In all of the cations, the two metals are bridged by two anionic cytosine ligands in a head–head fashion via the N3 donor (bound to Pt) and the singly deprotonated N4 amino ground (bound to Hg). The dinuclear cation of **1e** lies on a crystallographic symmetry mirror which, passing though Pt, Hg, N11, C11, N12, and C12, relates the two 1-MeC$^-$ ligands. The two cytosinate rings are almost coplanar, dihedral angles, being 6.8° (**1d**), 7.1° (**2d**), and 3.7° (**1e**). The coordination about Pt is completed by

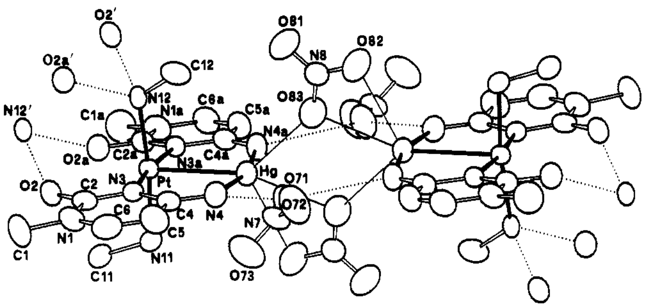

Figure 1. Centrosymmetric arrangement and labeling scheme of non-H atoms of **1d** (ORTEP drawing, 30% thermal ellipsoids). Dotted lines represent hydrogen bonds.

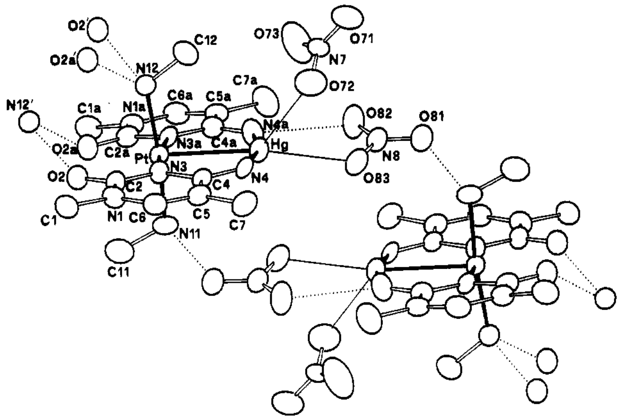

Figure 2. Centrosymmetric arrangement and labeling scheme of non-H atoms of **2d** (ORTEP drawing, 30% thermal ellipsoids). Dotted lines represent hydrogen bonds.

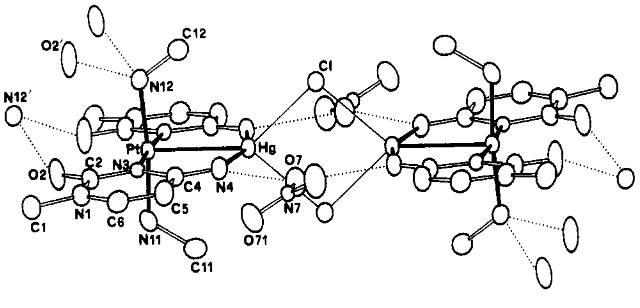

Figure 3. Centrosymmetric arrangement and labeling scheme of non-H atoms of **1e** (ORTEP drawing, 30% thermal ellipsoids). Dotted lines represent hydrogen bonds. Only one orientation of NO_3^- is shown.

Table VI. Selected Coordination Bond Lengths (Å) and Angles (deg) and Relevant Geometric Parameters for Structures **1d**, **2d**, and **1e**

	1d X = O83 Y = O82	**2d** X = O83 Y = O72	**1e**[a] X = Cl
Pt–Hg	2.785(1)	2.765(1)	2.835(1)
Pt–N3	2.036(8)	2.054(5)	2.035(6)
Pt–N3a	2.034(7)	2.019(5)	
Pt–N11	2.087(8)	2.053(6)	2.03(1)
Pt–N12	2.053(7)	2.041(6)	2.032(9)
Hg–N4	2.04(1)	2.033(6)	2.117(6)
Hg–N4a	2.03(1)	2.036(6)	
Hg–X	2.67(1)	2.769(5)	2.768(3)
Hg–X'	2.69(1)		2.752(3)
Hg–Y	2.70(1)	2.689(8)	
Hg–Pt–N3	85.8(2)	86.1(2)	87.9(1)
Hg–Pt–N3a	85.4(2)	86.6(1)	
Hg–Pt–N11	91.6(2)	89.6(2)	94.1(3)
Hg–Pt–N12	95.4(2)	96.4(2)	92.3(2)
N3–Pt–N3a	171.2(4)	172.7(2)	175.7(3)
N3–Pt–N11	91.2(3)	92.8(2)	89.5(1)
N3–Pt–N12	89.8(3)	88.8(2)	90.8(1)
N3a–Pt–N11	88.9(3)	87.6(2)	
N3a–Pt–N12	91.1(2)	91.5(2)	
N11–Pt–N12	173.0(3)	173.9(2)	173.6(2)
Pt–Hg–N4	82.0(3)	82.7(1)	78.1(2)
Pt–Hg–N4a	81.7(2)	81.4(2)	
Pt–Hg–X	157.8(2)	160.4(1)	136.32(6)
Pt–Hg–X'	136.9(3)		137.86(6)
Pt–Hg–Y	115.7(2)	127.1(2)	
N4–Hg–N4a	163.2(3)	164.1(2)	156.2(3)
N4–Hg–X	100.5(4)	111.1(2)	98.1(2)
N4–Hg–X'	95.2(5)		99.3(2)
N4–Hg–Y	96.5(4)	79.4(2)	
N4a–Hg–X	96.0(5)	84.4(2)	
N4a–Hg–X'	94.1(5)		
N4a–Hg–Y	94.0(5)	110.3(3)	
Y–Hg–X	42.2(3)	70.7(2)	
Y–Hg–X'	107.3(4)		
X–Hg–X'	65.2(4)		85.82(8)
Hg–X–Hg'	114.8(4)		94.18(8)
Hg···Hg'	4.523(1)	4.651(1)	4.043(1)
d(N3,N3a)[b]	0.14(1)	0.12(1)	0.090(5)
d(N11,N12)[b]	−0.14(1)	−0.12(1)	−0.098(9)
α[c]	6.8(9)	7.1(9)	3.7(2)

[a] N3a and N4a correspond to the atoms related by the symmetry mirror. [b] Displacement (Å) of N3, N3a (above) and N11, N12 (below) from the mean coordination PtN_4 plane. [c] Angle (deg) between the mean planes of the cytosinate anions.

two methylamine ligands and by Hg in the apical position of a square pyramid. Pt–Hg distances are 2.785(1) Å (**1d**), 2.765(1) Å (**2d**), and 2.835(1) Å (**1e**). Pt–N (with cytosinate and methylamine) bond lengths are normal, but angles about Pt display a distinct tetrahedral distortion of the PtN_4 coordination plane, as also indicated by the displacements of the four N donors out of the latter plane (Table VI).

To a first approximation, the Hg coordination in the cations is T-shaped, with two short distances to the N4 donors and a longer one to Pt. Mean Hg–N4 distances are in the range typical of deprotonated amine donors[31] and agree with distances found in $MeHg^{II}$ compounds with the metal-binding deprotonated amino groups of cytosine,[32] adenine,[33] and 8-azaadenine nucleobases[34] or HgL_2 complexes with L = deprotonated 1-methylthymine[35] and deprotonated cyclic amides.[36] The N4–Hg–N4a fragment is significantly bent, the angles at Hg being 163.2(3)° (**1d**), 164.1(2)° (**2d**), and 156.2(3)° (**1e**). In **1d** and **2d** the nitrate anions complete the Hg coordination sphere through long Hg–O distances. In **1d**, three O donors (O82, O83, O83') are approximately coplanar with Hg and Pt, thereby suggesting a hexacoordination of Hg, while in **2d**, two O donors (O72, O83) are virtually coplanar with the metal centers, providing two more equatorial ligands in a severely distorted trigonal bypramid (For examples of other irregular Hg coordination geometries, see refs 37 and 38). In the case of **1e**, two Cl^- ions bind Hg at distances of 2.768(3) and 2.752(3) Å and occupy two equatorial positions of a distorted bipyramid around Hg, the third equatorial ligand

---

(31) Brodersen, K.; Hummel, K.-U. In *Comprehensive Coordination Chemistry*; Wilkinson, G., Gillard, R. D., Mc Cleverty, J. A., Eds.; Pergamon Press: Oxford, U.K., 1987; Vol. 5, p 1047.

(32) Prizant, L.; Rivest, R.; Beauchamp, A. L. *Can. J. Chem.* **1981**, *59*, 2290.

(33) Olivier, M. J.; Beauchamp, A. L. *Acta Crystallogr.* **1982**, *B38*, 2159.

(34) Sheldrick, W. S.; Bell, P. *Inorg. Chim. Acta* **1986**, *123*, 181.

(35) (35)Kosturko, L. D.; Folzer, C.; Stewart, R. F. *Biochemistry* **1974**, *13*, 3949.

(36) (a) Goodgame, D. M. L.; Khaled, A. M.; Williams, D. J. *Polyhedron* **1991**, *10*, 1079. (b) Goodgame, D. M. L.; Khaled, A. M.; O'Mahoney, C. A.; Williams, D. J. *J. Chem. Soc., Chem. Commun.* **1990**, 851. (c) Goodgame, D. M. L.; Williams, D. J.; Winpenny, R. E. P. *J. Chem. Soc., Chem. Commun.* **1988**, 437 and references therein.

(37) Grdenic, D. *Q. Rev., Chem. Soc.* **1965**, *19*, 303.

(38) (a) Canty, A. J.; Marker, A.; Gatehouse, B. M. *J. Organomet. Chem.* **1975**, *88*, C31. (b) Deacon, G. B.; Raston, C. L.; Tunaley, D.; White, A. H. *Aust. J. Chem.* **1979**, *32*, 2195. (c) Kamenar, B.; Hergold-Brundic, A.; Sikirica, M. *Cryst. Struct. Commun.* **1976**, *5*, 149. (d) Halfpenny, J.; Small, R. W. H.; Thorpe, F. G. *Acta Crystallogr.* **1974**, *34B*, 3075. (e) Akesson, R.; Sandström, M.; Stalhandske, C.; Persson, I. *Acta Chem. Scand.* **1991**, *45*, 165.

being Pt and the two axial ones being N4 and N4a. The equatorial moiety of the bipyramid lies in the crystallographic mirror plane.

The $MeNH_2$ ligands in **1d** and **2d** are oriented in opposite directions (Figures 1 and 2) with respect to the remaining moiety of the cation. The C11 methyl group is on the O2 and O2a side nearly equidistant from these atoms (conformation A) while C12 points toward Hg (conformation B). The Hg–Pt–N11 and Pt–N11–C11 angles are 91.6(2) and 109.6(6)° in **1d** and 89.6(2) and 113.9(5)° in **2d**, respectively, while the corresponding numbers in the Hg–Pt–N12–C12 fragment are 95.4(2) and 119.4(7)° in **1d** and 96.4(2) and 120.3(5)° in **2d**, respectively. In **1e**, both of the methylamine ligands adopt conformation B. The Hg–Pt–N11 (92.3(2)°) and Hg-Pt-N12 (94.1(3)°) angles are similar as well as the Pt–N11–C11 (122.8(8)°) and Pt–N12–C12 (119.4(7)°) angles.

Tetranuclear Units. In the crystals of **1d**, pairs of dinuclear cations are bridged by four nitrate anions in such a way that tetranuclear units, arranged about crystallographic symmetry centers, are formed (Figure 1). The Hg···Hg′ distance is 4.523(1) Å, primed labels indicating atoms related by the symmetry center. The two symmetry-related N8 nitrate ions bridge Hg and Hg′, lying above and below the mean plane of the $Pt(1\text{-}MeC^-)_2Hg$ unit and with additional contacts, Hg–O82 of 2.70(1) Å, also acting as chelating ligands. The two symmetry-related N7 nitrates bridge the two cations through O71 by weak H-bonds to N4 (3.01(1) Å) and to N4′ (3.09(1) Å). A symmetry-related N7″ anion forms an additional weak H-bond O72″···N11 of 2.98(1) Å, in such a way to lead the N11 methylamine ligand to assume orientation A. The two $Pt(1\text{-}MeC)_2Hg$ units are nearly coplanar, Pt of one moiety being displaced 0.29 Å out of the plane of the other.

In **2d**, the N8 nitrate plane makes a dihedral angle of 17° with the $Pt(1,5\text{-}DimeC^-)_2Hg$ unit (Figure 2). Each of the two symmetry-related N8 nitrates bridges the two cations through a Hg–O83 contact (2.769(5) Å) and a H-bond O82···N4a (2.824(9) Å) with one cation and a H-bond O81···N11′ of 2.868(8) Å with the other. The latter H-bond induces orientation A in the N11 methylamine ligand. The presence of the cytosinate 5-methyl group does not allow the N7 nitrate to bridge the $Pt(1,5\text{-}DimeC^-)_2Hg$ units, as in **1d**. Therefore, this ion acts as a monodentate ligand coordinating Hg through O72 at a distance of 2.689(8) Å. The two $Pt(1,5\text{-}DimeC^-)_2Hg$ units are still parallel but are in a stairlike arrangement, so that Pt of one unit is displaced 3.20 Å out of the plane of the other (Figure 2). The Hg···Hg′ distance of 4.651(1) Å is very close to that found in **1d**.

The tetranuclear unit of **1e** is similar to that of **1d**, where the N8 nitrate ions are formally replaced by Cl^- anions. However, its symmetry, imposed by the crystallographic space group, is C_{2h} (Figure 3). The Hg_2Cl_2 fragment has an approximately diamond geometry with similar Hg–Cl distances (see above) and Hg–Cl–Hg and Cl–Hg–Cl′ angles of 94.18(8) and 85.82(8)°, respectively. As expected, the Hg–Cl distances are longer (≈0.3 Å) than those, ranging from 2.417(4) to 2.465(3) Å, reported for Hg compounds where Cl^- acts as monodentate ligand.[8b,39] Noticeably asymmetric Hg_2Cl_2 units, with two long and two short distances, have been found in other complexes.[40,41] The two symmetry-related N7 nitrate anions are arranged in positions similar to those found in **1d**, but lying along the crystallographic 2-fold axis with the N7–O7 bond, assuming two orientations with half-occupancy and differing by a rotation of 61(1)°. Another symmetry-related N7″ nitrate ion forms a H-bond O71″···N11 of 2.74(1) Å, imposing orientation B on the N11 methylamine ligand. The Hg···Hg′ distance of 4.043(1) Å in the tetramer is significantly shorter, by about 0.5 Å, than those found in **1d** and **2d** and corresponds to an increase of about 0.06 Å in the Pt–Hg distance and to a narrowing of about 8° in the N4–Hg–N4a angle (Table VI). Furthermore, the Hg–N4 distance of 2.117(6) Å in **1e** is significantly longer than the corresponding ones in **1d** and **2d**, which range from 2.03(1) to 2.04(1) Å.

Chart I

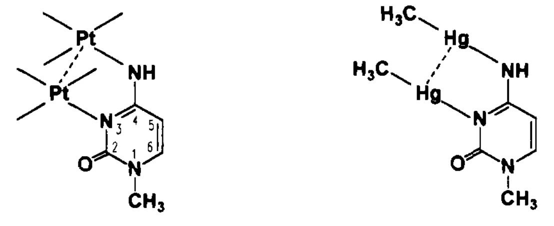

Pt^{II}----Pt^{II} 2.981 (2) Å Hg^{II}----Hg^{II} 3.150 (2) Å

Crystal Packing. In all the structures, the tetrameric units are held together by H-bonds between the N12 methylamine ligand of one tetramer and the O2′ and O2a′ oxygen atoms of the adjacent tetramer, as shown in Figures 1–3. These distances vary in the range 2.79–2.86 Å, in all three structures. This hydrogen-bond scheme imposes orientation B on the N12 methylamine ligand. The water molecule, with half-occupancy, in **2d** makes a hydrogen bond with O71 (2.79(1) Å).

Pt-Hg Interactions. Intracomplex Pt–Hg separations in our compounds are between 2.765(1) Å (**2d**) and 2.835(1) Å (**1e**). Among the structurally characterized mixed Pt–Hg compounds, there are examples with both longer[8b,9a,d] and shorter[8a,9b,c,42,43] intermetallic distances. As far as mixed-metal compounds derived from Pt^{II} and Hg^{II} are concerned, to which the following discussion shall be restricted, van Koten[8] has pointed out that these complexes can formally be divided into those with a short, covalent metal–metal bond (type I) and those with a considerably longer metal-to-metal donor bond (type II). A mixed Pt–Hg complex from van Koten's group[8b] with a single bridging ligand and a square-pyramidal coordination geometry of the Pt appears to have the closest similarity of all structurally characterized Pt^{II}–Hg^{II} compounds to our compounds. The compound, which is considered of type II, has a Pt→Hg donor bond of 2.8331(7) Å. On the basis of the van der Waals radii of Hg, 1.50 Å[35] to 1.73 Å,[44] and Pt, 1.70–1.80 Å,[45] a weak bonding interaction between the two metals in our Pt–Hg compounds may be anticipated. Comparison of these two heterodinuclear complexes with the closely related homodinuclear $[Pt^{II}]_2$ and $[Hg^{II}]_2$ species *cis*-$[(NH_3)_2Pt(1\text{-}MeC^-\text{-}N3,N4)_2Pt(NH_3)_2]^{2+}$ (*head–tail*)[46] and $[(CH_3Hg)_2(1\text{-}MeC^-\text{-}N3,N4)]^+$ [32] (Chart I) is instructive in this context. Since the metal–metal distances in these two homodinuclear compounds are not considered to imply any substantial bonding, a Pt–Hg distance of less than 0.5 (2.981 + 3.150) = 3.066 Å in a heteronuclear Pt–Hg complex of similar structure (**1d**, **1e**, **2d**) is indicative of bonding between the two metals.[47] Taking into account the very short Pt–Hg distances of 2.5–2.6 Å in some compounds, the 2.80-Å (average) distances in **1d**, **1e**, and **2d** indicate weak metal–metal bonds only (vide infra). Qualitatively, the bonding situation between Pt^{II} and Hg^{II} might described as in another d^8–d^{10} system between Ir^I and Au^I and bridging bis(diphenylphosphino)methane ligands.[4a] Depending

---

(39) Sharp, P. R. *Inorg. Chem.* **1986**, *25*, 4185.

(40) Averbuch-Pouchot, B. T.; El-Norr, N.; Guitel, J. C. *Acta Crystallogr.* **1984**, *C40*, 725.

(41) Johnson, B. F. J.; Kwik, W. L.; Lewis, J.; Raithby, P. R.; Saharan, V. P. *J. Chem. Soc., Dalton Trans.* **1991**, 1037.

(42) Bochkarev, M. N.; Ermolaev, N. L.; Zakharov, L. N.; Saf'Yanov, Yu N.; Razuvaev, G. A.; Struchkov, Yu. T. *J. Organomet. Chem.* **1984**, *270*, 289.

(43) Suleimanov, G. Z.; Bashilov, V. V.; Musaev, A. A.; Sokolov, V. I.; Reutov, O. A. *J. Organomet. Chem.* **1980**, *202*, C61.

(44) Canty, A. J.; Deacon, G. B. *Inorg. Chim. Acta* **1980**, *45*, L225.

(45) Bondi, A. *J. Phys. Chem.* **1964**, *68*, 441.

(46) Faggiani, R.; Lippert, B.; Lock, C. J. L.; Speranzini, R. A. *J. Am. Chem. Soc.* **1981**, *103*, 1111.

(47) In a trimethylphosphine analogue of cis-$[(NH_3)_2Pt(1\text{-}MeC^-)_2Pt(NH_3)_2]^{2+}$, the Pt–Pt separation is considerably larger, 3.199(2) Å, possibly due to steric interference between the $(CH_3)_3P$ groups. See: Trovó, G.; Bandoli, G.; Casellato, U.; Corain, B.; Nicolini, M.; Longato, B. *Inorg. Chem.* **1990**, *29*, 4616.

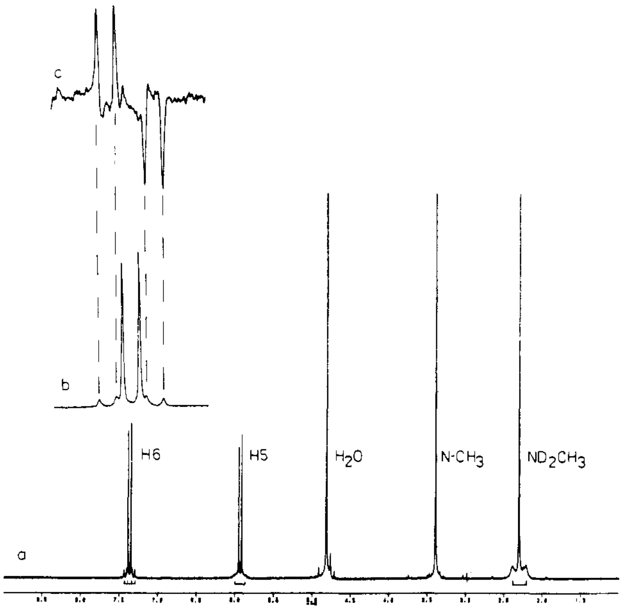

Figure 4. (a) ^{1}H NMR spectrum (D_2O, ambient temperature, pD 6.8) of **1d** with four ^{199}Hg satellites at H6, unresolved ^{195}Pt satellites at H5, and ^{195}Pt satellites at ND_2CH_3. A ^{199}Pt decoupling (not shown) leaves the H6 satellites while removing the others (not shown). (b) H6 resonance enlarged. (c) H6 resonance applying ^{199}Hg editing techniques.

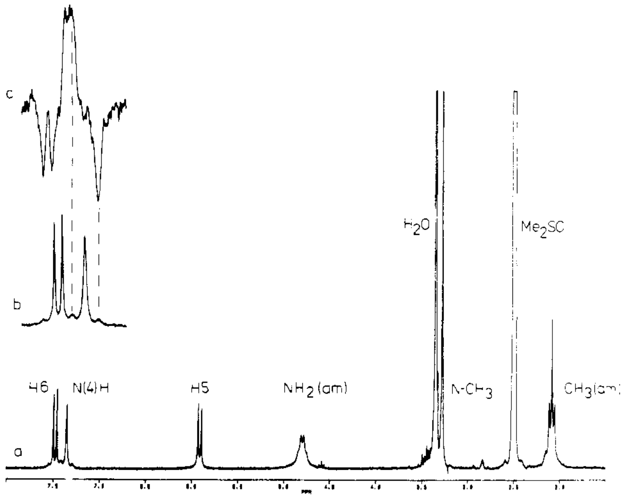

Figure 5. (a) ^{1}H NMR spectrum of **1d** in moist Me_2SO-d_6 (290 K). (b) H6 and NH(4) resonances enlarged with ^{199}Hg satellites at N(4)H and partially resolved ^{199}Hg satellites at H6. (c) ^{199}Hg edited ^{1}H NMR spectrum.

on relative energies of Pt^{II} and Hg^{II} orbitals and any possible mixing of orbitals of the respective metals (not determined in the present case), description as a weak metal–metal bond or as a donor–acceptor bond is possible.

NMR Studies. (i) ^{1}H NMR Spectra. As with the related Pt–Pd compounds,[24b] ^{1}H resonances of the cytosyl ligands in Pt–Hg complexes occur upfield from those of the corresponding bis(cytosine) complexes of *trans*-a_2Pt^{II}. This is primarily a consequence of nucleobase deprotonation. Metal binding to the deprotonated N4 position is expected to cause a partial downfield shift of cytosine resonances again. Since this effect is weaker than that of a proton, a net upfield shift is observed. ^{1}H NMR shifts (D_2O) of Pt–Hg compounds are given in the supplementary material. Consistent with a *head–head* arrangement of the cytosinato ligands in the Pt–Hg complexes, only a single set of 1-MeC$^-$ and 1,5-DimeC$^-$ resonances is observed. Upfield shifts of ^{1}H signals are approximately identical in the various Pt–Hg species, namely ca. 0.3 ppm for H6, 0.18 ppm for H5, and 0.09 ppm for $CH_3(1)$ of 1-MeC$^-$ compounds and ca. 0.30 ppm for H6, 0.08 ppm for $CH_3(1)$, and 0.05 ppm for $CH_3(5)$ in 1,5-DimeC$^-$ compounds. In Me_2SO-d_6, shifts of the nucleobase resonances are slightly different, with N(4)H and Pt–amine protons observable as well, e.g. at 7.23 ppm (N(4)H) and 4.08 ppm ($(NH_3)_2$) for **1c**. Occasionally, satellites due to coupling of ^{1}H with ^{195}Pt ($I = {}^1/_2$, 33.7% natural abundance) or ^{199}Hg ($I = {}^1/_2$, 16.9% natural abundance) is observed. Figure 4 provides the ^{1}H NMR spectrum of **1d** in D_2O. The CH_3 resonances of the ND_2CH_3 groups display ^{195}Pt coupling ($^3J \approx 38$ Hz), while satellites of the cytosyl H(5) doublet are broadened almost beyond resolution. The H6 doublet has four ^{199}Hg satellites of $^5J \approx 20$ Hz. Relative intensities of these satellites are close to expectations. In Me_2SO-d_6 (Figure 5), the cytosyl NH resonance at 7.36 ppm shows ^{199}Hg satellites ($^2J \approx 26$ Hz). The assignment of the satellites was confirmed both by a ^{195}Pt decoupling experiment, which leaves the ^{199}Hg satellites unaffected while wiping out the ^{195}Pt satellites, and by using spectral editing techniques. The H6 singlet[48] in the ^{1}H NMR spectrum of **2d** displays a pair of ^{199}Hg satellites of ^5J = 25 Hz (not shown). ^5J coupling between ^{199}Hg and H6 in the mixed Pt–Hg compounds thus is more than twice as large as with ^{195}Pt in *cis*-$[(NH_3)_2Pt(1\text{-}MeC^-)_2Pt(NH_3)_2]^{2+}$.[49]

Our observations of ^{199}Hg–^{1}H coupling with aromatic nucleobase protons appears to be the first report of its kind. While it is not surprising that—despite kinetic inertness—long-range ^{199}Hg–^{1}H coupling has not been observed in binary or ternary complexes of Hg^{II} with thymidinato-*N3* or guanosinato-*N1* ligands[50] or in labile CH_3Hg^+ complexes of guanosine or inosine,[51] it is surprising that in kinetically inert adeninato complexes of CH_3Hg^+ such coupling has not been observed.[52] At least for compounds with CH_3Hg bound to N6 in an anti orientation relative to H2, coupling could have been expected.[53] Possibly the high resonance frequency (400 MHz) prevented its observation, even though it did allow detection of ^2J coupling with N(6)H. The magnitude of this coupling (75 Hz) is, compared to that of **1d**, remarkably large and probably is a consequence of the higher s contribution of the two-coordinate Hg as compared to that in our compound.

(ii) ^{195}Pt NMR Spectra. ^{195}Pt NMR chemical shifts of *trans*-$[a_2PtL_2]^{2+}$ compounds are consistent with expections for Pt^{II} in a N_4 ligand system: –2598 ppm (**1a**), –2636 ppm (**1b**), –2597 ppm (**2a**), and –2636 ppm (**2b**). In the heteronuclear Pt–Hg compounds, the ^{195}Pt resonances are shifted to –2227 ppm (**1d**) and –2214 ppm (**2d**). Due to insufficient solubilities in water, ^{195}Pt spectra of the other Pt–Hg compounds were not obtained. The trend of ^{195}Pt shifts is thus comparable with the situation in mixed Pt–Pd compounds.[24b] Figure 6 shows the ^{195}Pt{^{1}H} NMR spectrum of **1d** in water. Satellites due to coupling with the ^{199}Hg isotope are to be seen. The magnitude of the ^1J coupling constant of 2783 Hz in **1d** and 2850 Hz in **2d** is a clear indication of direct Hg–Pt bonding, despite the somewhat long distances between the two metals as compared to Pt–Pd distances. These values compare with a reported 5087-Hz coupling in a Pt–Hg complex having a stronger metal–metal bond of 2.531 Å and a higher s contribution (sp hybridization of Hg).[9c] The ^{199}Hg chemical shifts of **1d** (–1162 ppm) and **2d** (–1163 ppm) have been determined in HMQC experiments. Because of the large line width in the Hg dimension (F1), Pt coupling was not resolved.

---

(48) The expected splitting into a quarted due to ^4J coupling with the methyl protons at C5 is not always well resolved.

(49) Lippert, B. *Gazz. Chim. Ital.* **1988**, *118*, 153.

(50) Buncel, E.; Boone, C.; Joly, H. *Inorg. Chim. Acta* **1986**, *125*, 167.

(51) (a) Canty, A. J.; Tobias, R. S. *Inorg. Chem.* **1979**, *18*, 413. *(b) Buncel, E.; Norris, A. R.; Racz, W. J.; Taylor, S. E. Inorg. Chem.* **1981**, *20*, 98.

(52) Charland, J. P.; Viet, M. T. P.; St. Jacques, M.; Beauchamp, A. L. *J. Am. Chem. Soc.* **1985**, *107*, 8202.

(53) With a syn orientation of CH_3Hg^+, coupling is expected to be considerably smaller and possibly not detected. This argument possibly also applies for similar complexes of 8-azaadenine ligands: Sheldrick, W. S.; Bell, P. *Inorg. Chim. Acta* **1989**, *160*, 265.

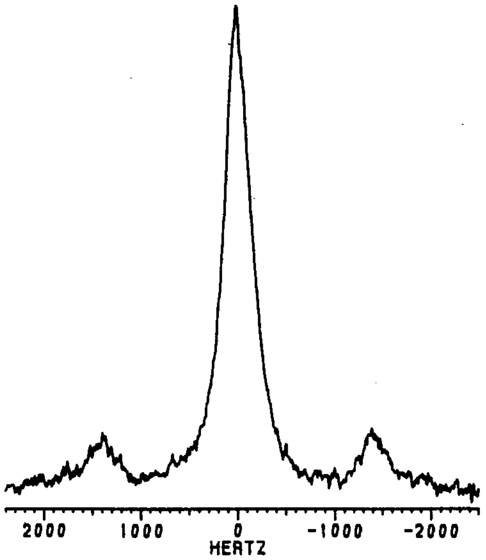

Figure 6. $^{195}Pt\{^1H\}$ NMR spectrum of **1d** (D_2O, pD 6.8) with ^{199}Hg satellites of ^1J = 2783 Hz.

Our attempt to observe the Hg resonance directly have been unsuccessful, probably because of unfavorable Hg relaxation behavior.

Reactivity. Reactivity patterns of Pt–Hg complexes, as established primarily by ^1H NMR spectroscopy, can be summarized as follows: (i) The compounds are inert on the NMR time scales (^1H, ^{195}Pt). Addition of increasing amounts of $Hg(NO_3)_2$ to the Pt–Hg complexes has no effect on any of the 1-MeC$^-$, 1,5-DimeC$^-$, or Pt resonances. Observation of ^{199}Hg coupling with ^{195}Pt and with H6 of 1-MeC$^-$ and 1,5-DimeC$^-$ is consistent with this interpretation. (ii) Pt–Hg compounds are stable toward HNO_3 down to pH 2. Below this pH, ligand protonation and complex decomposition take place:

$$trans\text{-}[a_2Pt(L^-)_2Hg]^{2+} + 2H^+ \rightarrow trans\text{-}[a_2PtL_2]^{2+} + Hg^{2+}$$

(iii) In a trans-metalation reaction, Pd^{II} (from K_2PdCl_4 or *trans*-$[(NH_3)_2Pd(H_2O)_2]^{2+}$) is capable of substituting Hg^{II}, with formation of PtPdY (Y = Cl$^-$ or NH_3).[24] (iv) Ligand substitution reactions (of NO_3^- or Cl$^-$) at Hg^{II} in Pt–Hg complexes are not nearly as versatile as those in Pt–Pd complexes.[24b] The following situations can be differentiated:

(a) No reaction. This applies to NH_3 (pH 10.5), L-alanine (pH 10.2), pyrazine (pH 8.2), and Me_2SO. Variations in relative concentrations have no effect.

(b) Decomposition according to

$$trans\text{-}[a_2Pt(L^-)_2Hg]^{2+} + 2X + 2H_2O \rightarrow trans\text{-}[a_2PtL_2]^{2+} + [HgX_2]^{2+} + 2OH^-$$

or

$$trans\text{-}[a_2Pt(L^-)_2Hg]^{2+} + 2X \rightarrow trans\text{-}[a_2PtL_2]^{2+} + Hg(X^-)_2$$

Frequently, the binary $HgX_2^{2+}/Hg(X^-)_2$ complex is poorly soluble and is not detected in ^1H NMR (D_2O) spectra, but the very soluble *trans*-$[a_2PtL_2]^{2+}$ complex is always readily recognized and identified. Reactions of this kind apply to the amino acids *N*-acetyl-L-histidine (pD 3.1 or 6.6), L-cysteine (pD 2.5 or 7.6), and L-methionine (pD 2.8)[54] and the nucleobases 1-methylthymine (pD 7.9 or pD 3), 1-methyluracil (pD 3), 1-methylcytosine (pD 6.5), 9-methyladenine (pD 2–3),[55] and 5′-guanosine monophosphate. Reactions with 2-thiouracil and urea likewise led to decomposition. In several cases, the precipitated binary Hg^{II} complexes were prepared by direct reaction of $Hg(NO_3)_2$ and X (X$^-$) and unambiguously identified by IR spectroscopy and elemental analysis (e.g. $Hg(1\text{-}MeT)_2$).

(c) Ligand Substitution. Apart from the chloro complex **1e**, only a single other compound with coordination of a ligand other than NO_3^- could be obtained. Reaction of **1d** with 1 equiv of NaSCN led to the precipitation of *trans*-$[(CH_3NH_2)_2Pt(1\text{-}MeC^-)_2Hg(SCN)]NO_3$ (**1f**). SCN$^-$ coordination is inferred from the shift of the IR active $\nu(C{\equiv}N)$ band from 2075 cm^{-1} (NaSCN) to 2089 cm^{-1} (**1f**). If SCN$^-$ is added in excess, complex decomposition according to section b and formation of $Hg(SCN)_2$ take place as evident from the appearance of ^1H NMR resonances due to **1b**.

Conclusion

In this report, we describe novel mixed-metal Pt–Hg complexes of the nucleobases 1-MeC and 1,5-DimeC. The binding patterns, as established in three crystal structure determinations, show Pt binding through N3 and Hg binding via deprotonated exocyclic amino groups of the nucleobases. The coordination geometry of Pt is that of a square pyramid with Hg sitting above a tetrahedrally distorted PtN_4 plane. In all three structures the coordination sphere of Hg is extended to coordination numbers 5 (**1e**, **2d**) and 6 (**1d**), respectively, with nitrate oxygens (**1d**, **2d**) or chloride (**1e**) being the additional ligands. These ligands, which all are located in the plane of distorted, compressed bipyramids (with Hg in the center and the N4 atoms at the vertices), affect the Pt···Hg separation: With Cl$^-$ (**1e**), the metal–metal distance is significantly longer than with O. Observation of strong coupling of ^{199}Hg with ^{195}Pt in Pt–Hg complexes is indicative of direct metal–metal bonding rather than an "interaction" between the two metals via the heterocyclic rings. As with the related Pt–Pd system, in which the d^8 entity Pt donates electrons to the d^8 entity Pd, the bonding situation in Pt–Hg systems could possibly be interpreted in terms of a dative bond formalism, from Pt^{II} (d^8) to Hg^{II} (d^{10}). This view[8] fits the metal–metal separations in our compounds, which are considerably longer than those in Pt–Hg compounds having a strong covalent bond. The reverse situation, dative bonding from d^{10} to d^8, as found in a Ni^0→Pd^{II} system,[56] is unlikely in that it would require the d_{z^2} orbital of Pt^{II} to be empty and the $d_{x^2-y^2}$ to be filled. Additional work is clearly required to clarify the metal–metal bonding situation.

Although inert on the ^1H and ^{195}Pt NMR time scales like Pt–Pd complexes, the Pt–Hg compounds are much more readily decomposed by a variety of ligands, including biologically relevant ones. Therefore, one of our initial hopes, namely to develop these Pt–Hg compounds as stains for specific structural entities of biomolecules, is unlikely to be achieved.

Acknowledgment. This work was supported by the Deutsche Forschungsgemeinschaft, the Fonds der Chemischen Industrie, and MURST, Rome.

Supplementary Material Available: Tables of complete crystallographic data, atomic coordinates, bond lengths and angles, thermal parameters, and H atom coordinates for **1d**, **1e**, and **2d** and a listing of ^1H NMR chemical shifts (14 pages). Ordering information is given on any current masthead page.

---

(54) Acidic pH values were chosen on purpose in order to protonate NH_2 of the amino acid.

(55) Reaction with 9-MeA is very complex. It appears that a mixed 1-MeC–9-MeA complex of *trans*-a_2Pt^{II} is formed as well.

(56) Ni, J.; Kubiak, C. P. *Inorg. Chem.* **1990**, *29*, 4345.